Lewis and Brønsted acid catalysis with AlMCM-41 and AlMMS: dependence on exchange cation

H.H.P. Yiu and D.R. Brown *

Centre for Applied Catalysis, Department of Chemical and Biological Sciences, University of Huddersfield, Huddersfield HD1 3DH, UK
E-mail: d.r.brown@hud.ac.uk

Received 15 July 1998; accepted 6 October 1998

Mesoporous solid acid catalysts based on AlMCM-41 and AlMMS have been prepared. The two catalysts exhibit similar unidimensional pore structures with hexagonal symmetries. AlMMS shows less long-range order than AlMCM-41 but is considerably easier to synthesise. The catalytic activities have been measured and compared in the Lewis-acid-catalysed alkylation of toluene with benzyl chloride, and the Brønsted-acid-catalysed alkylation of toluene with benzyl alcohol. Activities have been measured for catalysts ion-exchanged with H^+, Fe^{3+}, Al^{3+} and Na^+, and following thermal activation at temperatures of 150–350 °C. They have also been compared with K10, a mesoporous acid-treated clay catalyst. Results show that the acid-treated clay is the most active of the three catalysts in both reactions. For all catalysts, the Fe^{3+} forms exhibit the highest Lewis acid catalytic activities, and the Al^{3+} and H^+ forms show higher Brønsted acid activities. Infrared spectra of adsorbed pyridine show relative concentrations of Lewis and Brønsted acid sites consistent with this. Differences in the dependence of catalytic activities on thermal activation temperature are interpreted in terms of the hydration properties of the catalysts.

Keywords: MCM-41, MMS, mesoporous molecular sieve, solid acid, acid-treated clay, acid-activated clay, montmorillonite, acid catalysis, Lewis acidity, Brønsted acidity, alkylation

1. Introduction

A requirement for porous solid acid catalysts for use in liquid-phase processes is that the pores be large enough to allow rapid diffusion of reactants in and products out. This generally precludes microporous materials and means that the catalysts should be mesoporous (pore diameter > 2 nm). Until recently, ordered structures with pores of this size were difficult to synthesise, and the only readily available mesoporous solid acids were low-order materials such as acid-treated clays, with relatively broad and difficult-to-control pore size distributions. However, the discovery of the MCM mesoporous silicas [1,2] in 1992, into which lattice heteroatoms such as aluminium can readily be incorporated to impart cation exchange capacity, introduced the possibility of making more highly ordered, thermally stable, mesoporous solid acids.

The most widely studied example of these mesoporous molecular sieves is MCM-41 and lattice-substituted variants such as AlMCM-41. They exhibit a unidimensional pore structure with hexagonal symmetry, and many workers have studied the catalytic properties of acid forms of the materials [3,4]. It seems, however, that the acid strengths of catalysts based on AlMCM-41 are relatively low, and certainly lower than those of comparable (microporous) zeolites [5,6].

Various attempts have been made to increase the acid strengths of these molecular sieves. One approach involves a change in the synthesis conditions, replacing the cationic surfactant templates used in MCM-41 (or AlMCM-41) with non-ionic surfactants [7–9]. An example is the method of Mokaya and Jones [7,8] leading to materials identified as MMS and AlMMS. They can be prepared with similar hexagonal symmetry to MCM-41 and similar surface areas. The pore structures are also similar although, in order to prepare materials with comparable long-range order (in terms of XRD patterns), it is usually necessary to use smaller surfactants (typically, C_{12} compared to C_{16}), resulting in slightly smaller pores. Even then, MMS molecular sieves tend to be somewhat less well ordered than MCM-41.

As well as exhibiting acid sites of higher strength, an important advantage of AlMMS materials over conventional AlMCM-41 is that the product is synthesised in its acidic form directly. There is no need to carry out ion exchange with NH_4^+ followed by a (second) calcination to generate the H^+-exchanged catalyst [7].

The nature of the exchange cation clearly has a profound effect on both the acidities and the catalytic activities of both AlMCM-41 and AlMMS. However, reported catalytic studies using both types of catalyst have mainly been based on either H^+-exchanged or as-prepared materials [3–9]. The objective of this work has been to examine the influence of the exchange cation on acid strength and on catalytic activity in both AlMCM-41 and AlMMS. These catalysts have been compared with the commercially available acid-treated clay K10, which is a widely used catalyst in liquid-phase reactions [10–13].

Brønsted and Lewis acidities have been distinguished using two model liquid-phase batch reactions. The alkylation

* To whom correspondence should be addressed.

of toluene with benzyl alcohol has been used to monitor Brønsted acidity, and the same alkylation reaction using benzyl chloride to measure Lewis acidity. Attempts have been made to assess the relative concentrations of surface Lewis and Brønsted acid sites by infrared study of adsorbed pyridine [14].

2. Experimental

2.1. Preparation

The synthetic procedure of Klinowski et al. [15] was used for AlMCM-41 molecular sieves. Experiments reported here have been based on materials with a formal Si/Al ratio of 15. Tetramethylammonium hydroxide (5 g of 25% TMAOH, Aldrich) and sodium silicate (3.15 g of 28%, Aldrich) were added to 20 g water and stirred. Sodium hydroxide (0.57 g) was mixed with cetyltrimethylammonium chloride solution (17.62 g of 25% CTMACl in water) and added to the silicate solution with stirring. Fumed silica (2.26 g Cab-o-Sil M-5) was then added to the mixture and stirred for 2 h. A suitable amount of aluminium sulphate hydrate was dissolved in 5 cm^3 water and added to the mixture with stirring. The pH was adjusted to 11.5 with dilute sulphuric acid. The mixture was heated in a digestion bomb at 150 °C for 48 h. The AlMCM-41 precipitate was then recovered by suction filtration and air-dried. The samples were calcined in air at 540 °C for 6 h.

The synthetic method of Mokaya and Jones [7] was used for AlMMS molecular sieves and, again, experiments have been based on catalysts with a formal Si/Al ratio of 15. Tetraethylorthosilicate (98% TEOS, 8.33 g) was added to 16 cm^3 ethanol. An appropriate amount of aluminium tripropoxide was dissolved in 7 cm^3 isopropanol and added to the silicate solution. The mixture was heated to 70 °C for 4 h. The surfactant 1-dodecylamine (1.85 g) was dissolved in 10 cm^3 4 : 6 water/ethanol mixture and added to the cooled silicate mixture. The mixture was allowed to react with stirring for 20 h at room temperature. The solid was recovered by suction filtration and then air-dried for 24 h at room temperature. Dry samples were calcined at 650 °C for 4 h under air.

The acid-treated montmorillonite K10 was kindly supplied by Sud-Chemie.

Calcined AlMCM-41 and AlMMS were ion-exchanged with 1 $mol\,dm^{-3}$ solutions of the metal nitrates (Al^{3+}, Fe^{3+}, and Na^{+}) in a molar ratio of 1 : 40 at 90 °C for 4 h. The K10 clay was ion-exchanged with Fe^{3+} and Al^{3+} in the same way. Samples were filtered, washed with hot water, and air-dried. Exchange of AlMCM-41 with H^{+} was performed by ion exchanging with NH_4^{+} as above, followed by calcination at 540 °C for 20 h.

2.2. Characterisation

Specific surface areas (BET) and pore size distributions (BJH) were measured by N_2 adsorption/desorption at 77 K, and are based on the adsorption and desorption isotherms, respectively. Samples were out-gassed under vacuum at 250 °C (150 °C for K10) for 5 h prior to adsorption.

Powder X-ray diffraction patterns were recorded using Cu K_α radiation. Solid-state ^{27}Al MASNMR spectra were recorded on air-dried samples of AlMMS and AlMCM-41 at the EPSRC facility, University of Durham. Elemental analyses were performed by X-ray fluorescence at Sheffield Hallam University.

IR of adsorbed pyridine: self-supporting wafers, of between 20 and 30 mg, were prepared and evacuated to 10^{-3} Torr at 150 °C for 1 h. Pyridine vapour was admitted at room temperature for 2 h, followed by 1 h at 100 °C to ensure effective penetration by pyridine. Excess pyridine was pumped away at 100 °C until the pressure fell to 2×10^{-3} Torr. The wafers were moved into the IR beam while under vacuum and transmission FTIR spectra were recorded at room temperature. In each case, background spectra were recorded for the catalysts subject to the same activation but without treatment with pyridine. The reported spectra are, therefore, the difference spectra between those of catalysts with adsorbed pyridine and those of catalysts which received no exposure to pyridine.

2.3. Catalytic measurements

Alkylation of toluene with (i) benzyl chloride and (ii) benzyl alcohol

All reagents were anhydrous and of AnalaR grade and were stored over molecular sieve before use. The catalyst (250 mg for benzyl chloride reaction and 100 mg for benzyl alcohol reaction) was activated at either 150, 250 or 350 °C under flowing dry air for 1 h. The catalyst was cooled to the reaction temperature (50 °C for benzyl chloride and 80 °C for benzyl alcohol). Toluene/benzyl chloride or toluene/benzyl alcohol (10 g of mixture, 20 : 1 in mol), pre-heated to the reaction temperature, was added to the catalyst with stirring, maintaining the dry air flow. Samples were taken at 15 min intervals for 2 h, and analysed with GC, using tetradecane as an internal standard.

3. Results

3.1. Catalyst characterisation

3.1.1. N_2 adsorption/desorption

Pore size distributions, specific surface areas, pore volumes, and Si/Al ratios for the as-prepared AlMMS and AlMCM-41, and K10, appear in figure 1.

The two mesoporous molecular sieves show much higher surface areas and porosities than the K10, and narrower pore size distributions. The AlMMS shows a higher surface area and greater porosity than AlMCM-41, but slightly smaller pores, in line with the smaller surfactant template, and a less well defined pore size distribution.

The acid-treated clay K10 exhibits a relatively low surface area and pore volume, but a very broad pore size dis-

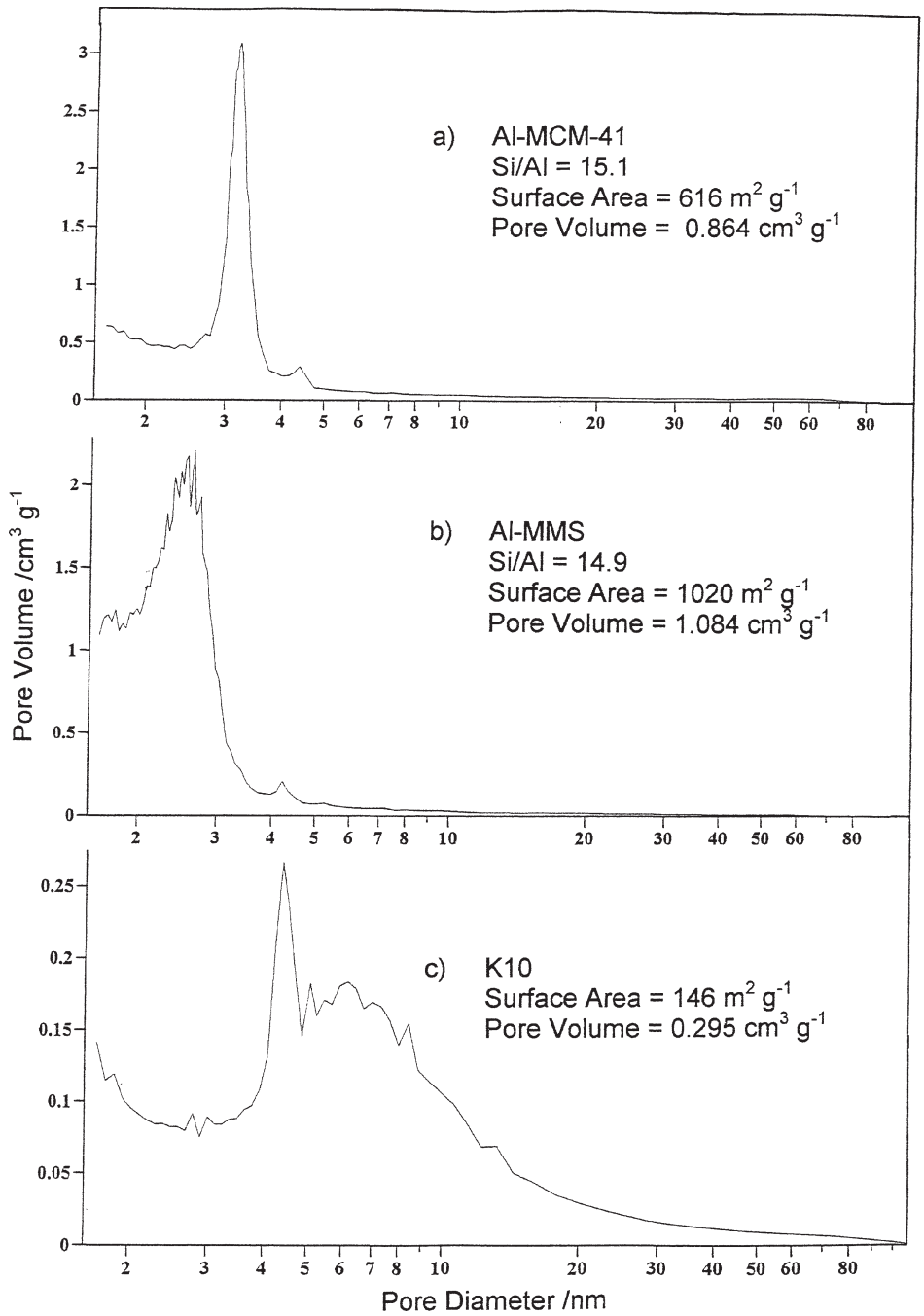

Figure 1. Pore size distributions based on N_2 desorption and the BJH method for as-prepared (a) AlMCM-41, (b) AlMMS and (c) K10 acid-treated montmorillonite. Si/Al ratios (XRF), specific surface areas and pore volumes (pore diam. $>$ 1.66 nm) are also shown.

tribution (note the expanded scale on the y-axis), with significant volume in pores of diameter greater than 10 nm. The narrow peak at around 4.5 nm is an artefact, characteristic of "expanding" clays. It is thought to be due to an abrupt rearrangement of the residual laminar clay structure accompanied by an expulsion of N_2 during the desorption leg of the isotherm [16,17].

3.1.2. XRD

The powder X-ray diffraction patterns for as-prepared AlMMS and AlMCM-41 are shown in figure 2. Both show clear reflections from 100 planes, representing d_{100} spacings for AlMCM-41 of 4.4 nm and for AlMMS 4.0 nm. This spacing multiplied by $2/\sqrt{3}$, giving 5.1 and 4.6 nm, is equal to one pore diameter plus the thickness of one pore wall [18]. Comparing these values with the maxima in the pore size distributions (3.2 and 2.7 nm) gives an indication of the wall thickness in the two lattices. Neither diffraction pattern is well resolved but the peaks are narrower for AlMCM-41 and higher-order reflections are just visible, suggesting that this material is slightly more highly ordered than AlMMS.

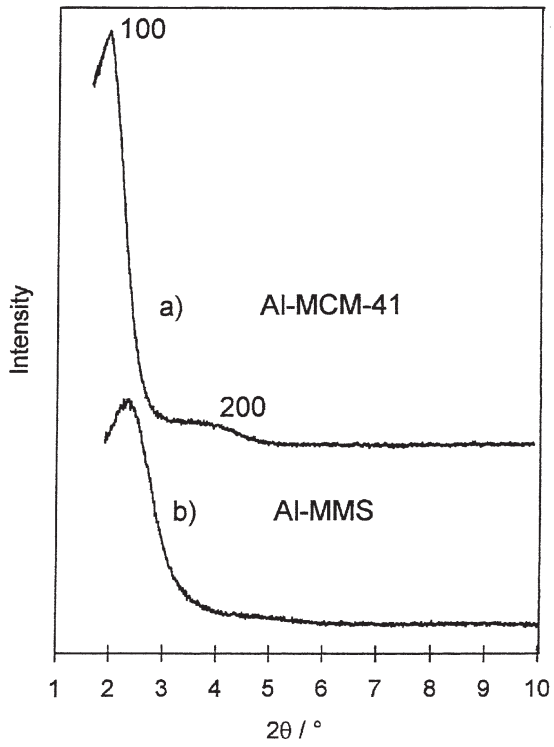

Figure 2. Powder XRD patterns for air-dried, as-prepared (a) AlMCM-41 and (b) AlMMS.

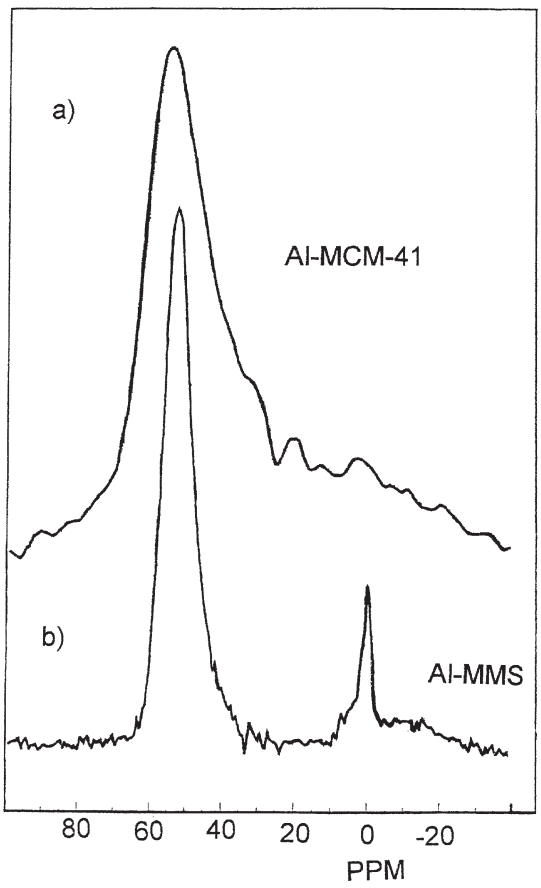

Figure 3. ^{27}Al MASNMR spectra of as-prepared (a) AlMCM-41 and (b) AlMMS.

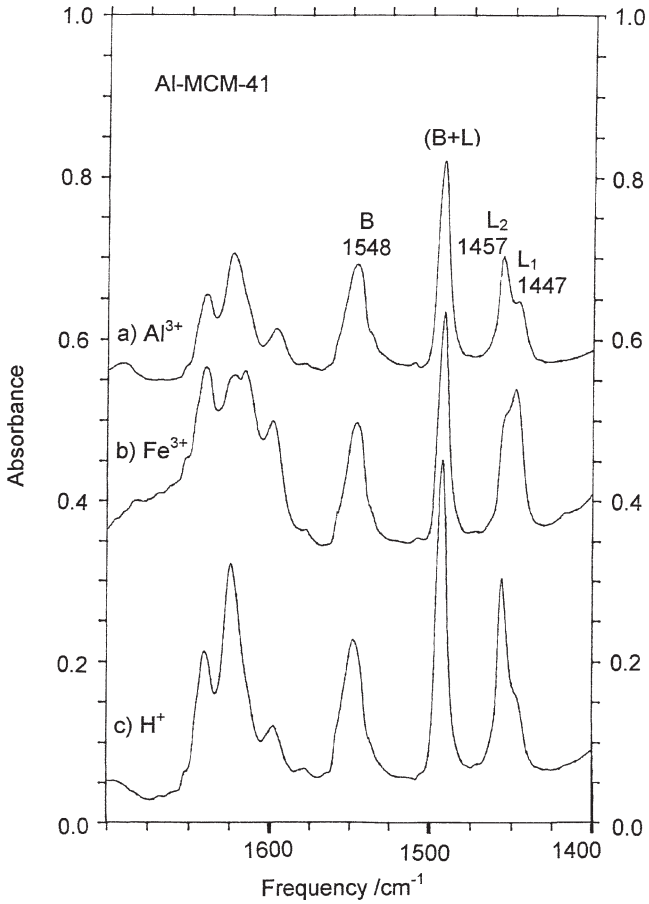

Figure 4. FTIR difference spectra of adsorbed pyridine on AlMCM-41, ion-exchanged with (a) Al^{3+}, (b) Fe^{3+} and (c) H^+. Catalyst samples were activated at 150 °C before exposure to pyridine and evacuated at 100 °C following exposure. Bands associated with Lewis acid sites (L) and Brønsted acid sites (B) are shown.

3.1.3. ^{27}Al MASNMR

Spectra of the same two materials, AlMCM-41 and AlMMS, are shown in figure 3. The features at 0 ppm are associated with octahedrally coordinated (and, therefore, non-lattice) aluminium. The signals at 50–55 ppm are due to tetrahedrally coordinated aluminium in lattice sites. Incorporation of aluminium in lattice sites appears to be almost complete for both materials, with possibly better defined environments for lattice aluminium atoms in AlMMS.

3.1.4. IR of adsorbed pyridine

The infrared difference spectra of adsorbed pyridine on AlMCM-41 exchanged with H^+, Al^{3+} and Fe^{3+} are shown in figure 4. The band at 1548 cm^{-1} is associated with the pyridinium ion formed when pyridine reacts with a Brønsted acid site, and the bands at 1440–1460 cm^{-1} are associated with pyridine coordinatively bound to Lewis acid sites [14]. In uncoordinated pyridine the equivalent band appears at 1438.5 cm^{-1}, and the stronger the Lewis acid site, the more this band is shifted to higher frequency.

A measure of the concentrations of Brønsted and Lewis sites (in arbitrary units) is made by dividing the integrated

Table 1
Relative concentrations of Lewis and Brønsted acid sites on AlMCM-41 catalysts, based on infrared spectral intensities.

Catalyst	Conc. Lewis acid sites (arb. units)	Conc. Brønsted acid sites (arb. units)
H^+ AlMCM-41	1.74	2.38
Al^{3+} AlMCM-41	1.68	2.46
Fe^{3+} AlMCM-41	1.92	2.21

absorbances in the two regions by the weights of the wafers, and by the molar absorptivities, 1.67 ($cm\,mmol^{-1}$) for Brønsted and 2.22 for Lewis acid sites [19]. These concentrations appear in table 1. They show that the Fe^{3+} catalyst has the highest concentration of Lewis acid sites, and the Al^{3+} and H^+ catalysts have higher concentrations of Brønsted acid sites.

All three catalysts show two close, but distinct, bands in the 1440–1460 cm^{-1} Lewis acid region rather than a single band as might be expected. For each catalyst, the two bands, labelled L_1 and L_2, appear at the same frequencies, 1447 and 1457 cm^{-1}, but with different relative intensities. The higher frequency 1457 cm^{-1} line dominates in the H^+- and Al^{3+}-exchanged materials, but the lower frequency 1447 cm^{-1} line dominates in the case of the Fe^{3+}-exchanged AlMCM-41.

3.2. Catalytic activities

Brønsted acid catalytic activities have been measured using the alkylation of toluene with benzyl alcohol. The major products are 1,2- and 1,4-methyldiphenylmethane. Activities are reported in terms of pseudo-first-order rate constants for the conversion of benzyl alcohol. In all cases a small amount of dibenzylether was also formed. However, the relative yield of this minor product was approximately the same in all cases, and its formation does not cause any significant deviation from first-order kinetics.

Lewis acid catalytic activities have been measured using the alkylation of toluene with benzyl chloride. The only products detected in this reaction are 1,2- and 1,4-methyldiphenylmethane, and activities are reported as pseudo-first-order rate constants for the conversion of benzyl chloride.

The rate constants for AlMCM-41 and AlMMS catalysts, exchanged with H^+ (AlMMS is generated in this form without further ion exchange), Na^+, Fe^{3+} and Al^{3+}, are shown in figure 5 for the Lewis-acid-catalysed reaction and figure 6 for the Brønsted-acid-catalysed reaction. Data is included for the acid-treated montmorillonite K10, ion-exchanged with Al^{3+} activated at 150 °C, and Fe^{3+} activated at 250 °C. Previous work has shown that K10 generates maximum Brønsted and Lewis acid activities with these exchangeable cations, respectively, and on activation at these temperatures [20,21].

3.2.1. Lewis acid catalysis (figure 5)

The most active Lewis acid catalyst in the series is the Fe^{3+}-exchanged acid-treated clay K10. Of the AlMMS and

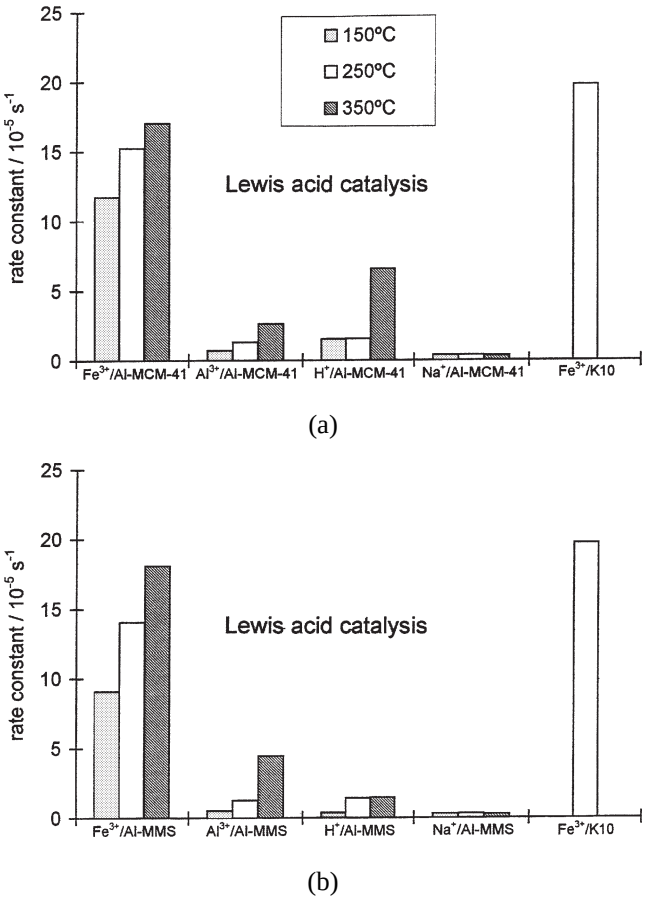

Figure 5. Pseudo-first-order rate constants for the alkylation of toluene with benzyl chloride, with ion-exchanged (a) AlMCM-41 and (b) AlMMS catalysts, and K10. Rate constants following thermal activation at 150, 250 and 350 °C are shown.

AlMCM-41 molecular sieve catalysts, it is also the Fe^{3+}-exchanged forms that are most active, with both showing maximum activities only slightly lower than K10.

The catalytic activities of the molecular sieves are very much more dependent on thermal activation than K10, which requires only 250 °C for maximum catalytic activity [20]. For both molecular sieve catalysts, the activities continue to rise as the activation temperature is increased up to 350 °C and quite possibly beyond. There is a difference in the way the two molecular sieves respond to increasing the activation temperature, with Fe^{3+}-exchanged AlMMS showing a considerably steeper rise in catalytic activity than the equivalent AlMCM-41 catalyst.

The Al^{3+} forms of both AlMMS and AlMCM-41 show low Lewis acid activities. The H^+ forms are similar, although the activity of H^+-exchanged AlMCM-41 increases dramatically on thermal activation at 350 °C. Catalysts in the Na^+ form show negligible activity, providing confirmation that the exchangeable cations are indeed the active sites.

3.2.2. Brønsted acid catalysis (figure 6)

The K10 acid-treated clay in the Al^{3+}-exchanged form is by far the most active of the catalysts tested in the Brønsted-

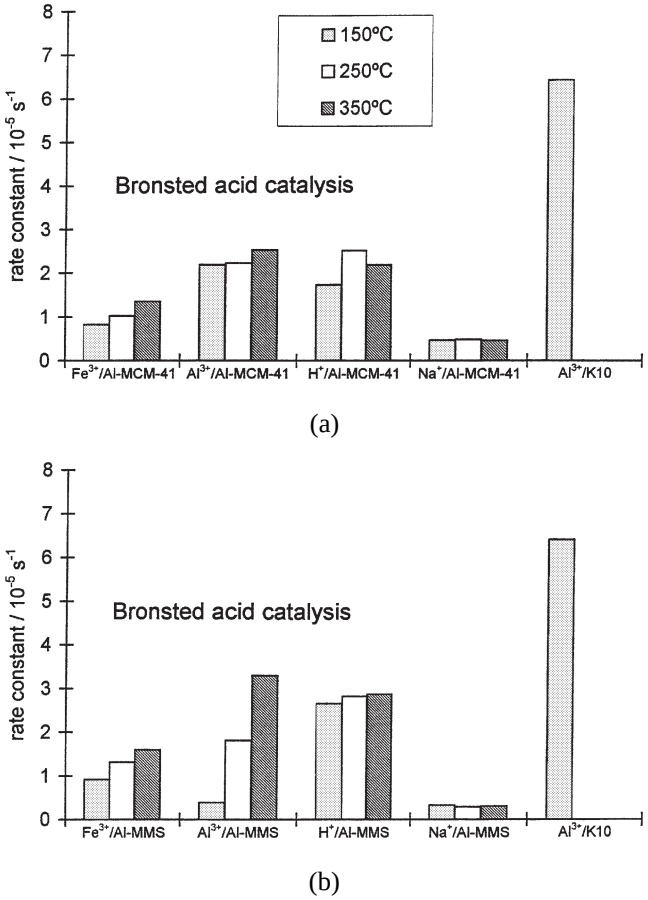

Figure 6. Pseudo-first-order rate constants for the alkylation of toluene with benzyl alcohol, with ion-exchanged (a) AlMCM-41 and (b) AlMMS catalysts, and K10. Rate constants following thermal activation at 150, 250 and 350 °C are shown.

acid-catalysed reaction. The much less active molecular sieve catalysts also show maximum activities in their Al^{3+} and H^+ forms. (H^+-exchanged clays are generally unstable [22], so direct comparisons using this cation are not possible.)

Again, maximum activities of the molecular sieve catalysts are reached at much higher thermal activation temperatures than K10. Where K10 exhibits maximum activity at 150 °C, falling at higher temperatures [20], the molecular sieve catalysts show Brønsted acid activities which continue to rise up to 350 °C and possibly beyond. As with the Lewis acid activity, it seems that the AlMMS catalyst, particularly in the Al^{3+} form, shows the more pronounced dependence on thermal activation temperature.

4. Discussion

4.1. Lewis acid catalysis

The most striking observation is that the acid-treated clay K10 shows higher catalytic activity than either of the mesoporous molecular sieves, and at a lower activation temperature. This difference in activity is made more remarkable by the lower cation exchange capacity (CEC), and, hence, concentration of acid sites, of the acid-treated clay. For K10, the CEC is estimated to be 0.2–0.4 mmol g^{-1} (based on the elemental analysis, assuming that CEC falls on acid treatment in proportion to the lattice Mg content; supported by data in [23]), and for AlMMS and AlMCM-41, based on the lattice aluminium content, about 1.0 mmol g^{-1}. The implication of this is that the Lewis acid sites in K10 are either very much more accessible in this kind of reaction medium, or much stronger, than those on AlMMS and AlMCM-41.

The importance of active site accessibility in catalysts of this type has been illustrated by Pinnavaia and Butruille, who studied similar reactions catalysed by K10 and a series of pillared clays [24]. They found evidence for diffusion control in the pillared clay catalysts and argued that the superior activity of the K10 was due largely to its wider pores and more accessible acid sites. Although the AlMMS and AlMCM-41 catalysts used here exhibit larger pores than the pillared clays, it is still likely that diffusion control is more important in these catalysts than in K10. However, it is significant that, in general, AlMMS catalysts show higher activities than AlMCM-41 catalysts, despite having slightly smaller pores, suggesting that diffusion control is not the overriding process limiting catalytic activity even in the molecular sieve catalysts.

In all three catalysts, the Fe^{3+}-exchanged forms are the most active Lewis acid catalysts. The Lewis acidity of this cation depends on its being largely dehydrated and on its interaction with the aluminosilicate surface. The molecular sieve catalysts seem to need much higher temperatures to dehydrate the Fe^{3+} ion than is needed by the acid-treated clay. This is particularly true of AlMMS catalysts, which appear to be more difficult to dehydrate than AlMCM-41, although it is worth noting that the ultimate catalytic activity achievable with Fe^{3+}-exchanged AlMMS is significantly higher than that of the equivalent AlMCM-41 catalyst.

The H^+ forms of both molecular sieve catalysts show low Lewis acid activities. This is not surprising since the mechanism by which H^+-exchanged catalysts develop Lewis acidity probably involves the elimination of water from the catalyst lattice. This does not seem to occur in H^+-exchanged AlMMS over the temperature range studied, but figure 5(a) suggests that it could be happening with H^+-exchanged AlMCM-41 at the highest activation temperature. This may be an indicator that AlMMS is more thermally stable than AlMCM-41. It may also be related to the greater resistance to dehydration of AlMMS over AlMCM-41 catalysts.

4.2. Brønsted acid catalysis

The acid-treated clay K10 is again the most active of the three catalysts in the Brønsted-acid-catalysed reaction. The explanation is probably the same as that for Lewis acid catalytic activity and must lie either in the strength or the accessibilities of the surface acid sites.

For all three catalysts, the Al^{3+} forms are the most active. For the exchangeable Al^{3+} ions, to generate maxi-

mum Brønsted acidity they must be only partially hydrated so that the ion's ability to polarise directly coordinated water molecules is maximised [25]. The results suggest that this optimum level of hydration is reached at much higher activation temperatures with the molecular sieves than with the acid-treated clay. This is consistent with the temperature dependence of Lewis acid activity for the Fe^{3+} forms of these catalysts described above.

The Brønsted acid activities of the Al^{3+}-exchanged molecular sieves show the same trends as are seen in the Lewis acid activities of the two Fe^{3+}-exchanged molecular sieve catalysts. The AlMMS catalyst shows the greater dependence on thermal activation temperature, ultimately exhibiting the higher activity of the two, but only on high-temperature activation.

The H^+ forms of the molecular sieves also show high Brønsted acid activities, as might be expected. It is reasonable to suggest that the activities of the H^+ forms of these catalysts, in effect, represent the maximum activities that might be achievable on dehydration of the Al^{3+} forms.

With AlMCM-41, the activities of the Al^{3+} and H^+ forms are similar at all activation temperatures between 150 and 350 °C. This is significant because it shows that maximum Brønsted acid catalytic activity can be achieved with AlMCM-41 by the relatively simple process of Al^{3+} exchange, without the need for the relatively complex procedure needed for H^+ exchange.

In contrast, it is more difficult to activate Al^{3+}-exchanged AlMMS and the catalytic activity only matches that of the H^+ form at 350 °C. This is less significant, however, because AlMMS is synthesised directly in the H^+ form and there is no advantage in being able to use the Al^{3+}-exchanged form for catalysis.

4.3. Lewis and Brønsted acid sites

The infrared spectra of adsorbed pyridine are consistent with the catalytic data, showing a higher concentration of Lewis acid sites in the Fe^{3+}-exchanged catalyst and higher relative concentrations of Brønsted acid sites in Al^{3+}- and H^+-exchanged catalysts.

The other significant observation from the spectra is the detection of two bands, rather than one, in the Lewis acid 1440–1460 cm^{-1} region. Similar pairs of bands at virtually the same frequencies have been previously reported for pyridine adsorbed on zeolites [26], other oxides [27] and on some acid-treated clays [28]. These pairs of bands have invariably been interpreted in terms of two discrete types of Lewis acid site. This may well be the explanation in this case although, intuitively, it seems a little unlikely that two types of well defined acid site, of very similar strengths, would exist together in such a diverse range of materials.

Further doubt on the assignment to two types of Lewis acid site arises because the apparently stronger of the two sites (1457 cm^{-1}) seems to be more abundant in the less active catalysts, and the weaker site (1447 cm^{-1}) dominates in the most active, Fe^{3+}-exchanged, AlMCM-41. The reverse might have been expected. Overall, we suspect that the reason for the splitting in the Lewis acid band may be different, although at this stage no alternative explanation is offered.

5. Conclusion

The acid-treated montmorillonite K10 can be used as a yardstick for new mesoporous acid catalysts for liquid-phase reactions. Those examined here are very much less active than the clay. This may be because the average strength of acid sites on K10 is higher than those on AlMMS and AlMCM-41, or it may be that K10 exhibits a broader distribution of acid site strengths than the more ordered molecular sieve catalysts, and a small number of highly active sites might then have a disproportionate effect on the overall activity.

Alternatively the high activity may be due to the accessibility of the acid sites. Even though the surface area of K10 is relatively small, the broad pore size distribution means that many of the acid sites will be in pores very much larger than those in AlMCM-41 and AlMMS, and facile diffusion to and from these sites may be the key to its high activity. An objective of further work is to establish whether the rates of typical liquid-phase reactions on this type of catalyst are diffusion controlled, and whether larger pore MCM- and MMS-based catalysts could reasonably be expected to show higher activities.

An important potential advantage of the structurally ordered MCM-41 and MMS materials over the disordered acid-treated clay is the reaction selectivities which might be achievable. No conclusions about this can be drawn from this work, although the better ordered AlMCM-41 might reasonably be expected to exhibit more shape selectivity than AlMMS.

Otherwise, AlMMS catalysts seem to show advantages over AlMCM-41, in terms of both catalytic activity and, particularly, ease of synthesis. AlMMS is prepared without the need for elevated pressure, and the as-prepared catalyst is in the H^+ form, without any need for further ion exchange. Even so, it is clear that there are still major advances to be made in the development of this class of acidic mesoporous molecular sieve catalyst, if they are to become commercially useful in acid-catalysed, liquid-phase processes.

Acknowledgement

Our thanks are due to Dr. Jenny Jones of the Department of Fuel and Energy, University of Leeds, for providing the facilities for the FTIR measurements and for help and advice in running and interpreting the spectra. Thanks are also due to Dr. Chris Breen, of the MRI, Sheffield Hallam University, for providing XRF measurements. The University of Durham EPSRC Solid-State NMR Service is kindly

acknowledged for providing MASNMR spectra. The University of Huddersfield is kindly acknowledged for a studentship for HHPY.

References

[1] C.T. Kresge, M.E. Leonowicz, W.J. Roth, J.C. Vartuli and J.S. Beck, Nature 359 (1992) 710.
[2] J.S. Beck, J.C. Vartuli, W.J. Roth, M.E. Leonowicz, C.T. Kresge, K.O. Schmitt, C.T.-W. Chu, D.H. Olsen, E.W. Sheppard, S.B. McCullen, J.B. Higgins and J.L. Schlenker, J. Am. Chem. Soc. 114 (1992) 10834.
[3] A. Corma, Chem. Rev. 97 (1997) 2373.
[4] J.S. Beck and J.C. Vartuli, Curr. Opin. Solid State Mater. Sci. 1 (1996) 76.
[5] R. Mokaya, W. Jones, Z. Luan, M.D. Alba and J. Klinowski, Catal. Lett. 37 (1996) 113.
[6] A. Corma, V. Fornes, M.T. Navarro and J. Perez-Pariente, J. Catal. 148 (1994) 569.
[7] R. Mokaya and W. Jones, J. Catal. 172 (1997) 211.
[8] R. Mokaya and W. Jones, J. Chem. Soc. Chem. Commun. (1996) 981.
[9] S.A. Bagshaw, E. Prouzet and T.J. Pinnavaia, Science 269 (1995) 1242.
[10] C. Cativiela, J.I. Garcia, M. Garcia-Matres, J.A. Mayoral, F. Figueras, J.M. Fraile, T. Cseri and B. Chiche, Appl. Catal. A 123 (1995) 273.
[11] A. Cornelis, A. Gerstmans, P. Laszlo, A. Mathy and I. Zieba, Catal. Lett. 6 (1990) 103.
[12] A. Cornelis and P. Laszlo, Acc. Rapid Commun. Synth. Org. Chem. (1994) 155.
[13] D.R. Brown, Geol. Carpath. Ser. Clays 1 (1994) 45.
[14] E.P. Parry, J. Catal. 2 (1963) 371.
[15] Z. Luan, C.-F. Cheng, W. Zhou and J. Klinowski, J. Phys. Chem. 99 (1995) 1018.
[16] S.J. Gregg and K.S.W. Sing, *Adsorption, Surface Area and Porosity* (Academic Press, London, 1980).
[17] C.N. Rhodes and D.R. Brown, J. Chem. Soc. Faraday Trans. 89 (1993) 1387.
[18] B. Marler, U. Oberhagemann, S. Vortmann and H. Gies, Micropor. Mater. 6 (1996) 375.
[19] C.A. Emeir, J. Catal. 141 (1993) 347.
[20] C.N. Rhodes and D.R. Brown, Catal. Lett. 45 (1997) 35.
[21] T. Cseri, S. Bekassy, F. Figueras and S. Rizner, J. Mol. Catal. A 98 (1995) 101.
[22] C.N. Rhodes and D.R. Brown, J. Chem. Soc. Faraday Trans. 91 (1995) 1031.
[23] D.R. Brown and C.N. Rhodes, Thermochim. Acta 294 (1997) 33.
[24] J.-R. Butruille and T.J. Pinnavaia, in: *Multifunctional Mesoporous Inorganic Solids*, NATO ASI Series C, Vol. 400, eds. C.A.C. Sequeira and M.J. Hudson (1993) p. 259.
[25] J.P. Rupert, W.T. Granquist and T.J. Pinnavaia, in: *Chemistry of Clays and Clay Minerals*, ed. A.C.D. Newman (Mineral. Soc., London, 1987) p. 275.
[26] M. Jiang and H.G. Karge, J. Chem. Soc. Faraday Trans. 91 (1995) 1845.
[27] D. Ballivet, D. Barthomeuf and P. Pichat, J. Chem. Soc. Faraday Trans. 68 (1972) 2027.
[28] F. Kooli and W. Jones, Clay Miner. 32 (1997) 633.